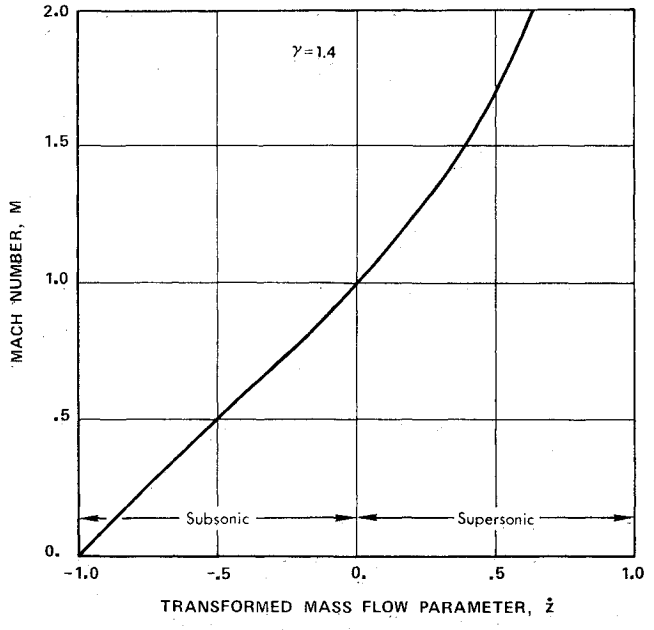

Fig. 2 Mach number variation with transformed total pressure mass flow parameter.

In many situations, however, $\dot{m}_s$ or $\dot{m}_t$ is known, and one needs to determine the Mach number. Equation (1) has a closed form inverse which can be written as

$$M^2 = -\frac{1}{\gamma-1} + \left[\left(\frac{1}{\gamma-1}\right)^2 + \frac{2R\dot{m}_s^{\,2}}{\gamma g(\gamma-1)}\right]^{1/2} \tag{3}$$

The equation has another root that corresponds to a negative M^2 which is physically unreal. A closed form solution for Eq. (2), however, is formidable. One usually resorts to the interpolation of tables, curves, or for machine computations, iterative schemes. Due to the infinite slope of the Mach number with respect to the mass flow parameter at the sonic point, however, one usually encounters the problem of numerical singularity. That is, the solution is difficult to obtain near $M = 1$. Using the Newton method of iteration, for example, one can reliably obtain a solution only up to a Mach number of about 0.9 in the subsonic region.

It has been found that such numerical singularity can be overcome by rewriting Eq. (2) in terms of a simple transformed mass flow parameter which is defined as

$$\dot{z} = \begin{cases} + \left(1 - \dfrac{\dot{m}_t}{\dot{m}_{t,\,\text{choke}}}\right)^{1/2} & M > 1.0 \\ - \left(1 - \dfrac{\dot{m}_t}{\dot{m}_{t,\,\text{choke}}}\right)^{1/2} & M < 1.0 \end{cases} \tag{4}$$

where $\dot{m}_{(t)\text{choke}}$ is the mass flow parameter at the sonic or choking condition. Thus, Eq. (2) becomes

$$\dot{z} = \pm \left\{1 - M\left[\frac{2+(\gamma-1)M^2}{\gamma+1}\right]^{-\frac{\gamma+1}{2(\gamma-1)}}\right\}^{1/2} \tag{5}$$

Where (+) and (−) are for supersonic and subsonic flows, respectively. The Mach number variation with respect to the transformed mass flow parameter $\dot{z}$ for air is plotted in Fig. 2. The transformed relationship has two distinctive advantages: 1) The infinite slope at $M = 1$ has disappeared, thus, eliminating numerical problems near $M = 1$. 2) The curve is nearly linear in the subsonic region, and thus one may closely approximate the Mach number by the relation

$$M \approx 1 - \dot{z}^2 \qquad 0 < M < 1.0 \tag{6}$$

In fact, Eq. (6) is exact for $\gamma = 1$. Thus, in any iterative scheme, Eq. (6) can be used as a close first approximation.

The inverse solution of Eq. (5) is ideal for the Newton iterative scheme, where successive approximations to the Mach numbers are given by

$$M_{i+1} = M_i - (\dot{z}_i - \dot{z})\left(\frac{dM}{d\dot{z}}\right)_i \tag{7}$$

where

$$\left(\frac{dM}{d\dot{z}}\right)_i = \frac{2\dot{z}_i\left[\dfrac{2+(\gamma-1)M_i^2}{\gamma+1}\right]^{\frac{\gamma+1}{2(\gamma-1)}}}{\dfrac{(\gamma+1)M_i^2}{2+(\gamma-1)M_i^2} - 1} \tag{8}$$

The derivative $dM/d\dot{z}$ is indeterminate at $M = 1.0$ but can be determined by the L'Hospital's rule. In this case

$$\lim_{M\to 1.0} \frac{dM}{d\dot{z}} = \frac{\gamma+1}{2} \tag{9}$$

Therefore, one should avoid the iteration when $\dot{z} = 0$. For such a case, however, the solution is known.

Transonic Flow around Symmetric Aerofoils at Zero Incidence

D. Nixon*
Queen Mary College, University of London, London, England

Introduction

ONE of the earliest attempts to treat the problem of mixed flows at transonic speeds was the integral method of Spreiter and Alksne[1] based on the nonlinear transonic small disturbance equation. This technique was developed in 1954 before the days of high speed computors and consequently involves a minimum of numerical work. Results obtained for circular-arc aerofoils at zero incidence compare unfavourably with the result of the more recent numerical methods[2-4] particularly as regards the shock location. The unsatisfactory nature of the results of Ref. 1 are a direct consequence of approximations introduced into the fundamental integral equation in order to simplify the numerical work. In this note it is shown that the introduction of a simple correction factor, depending only on the transonic similarity parameter, improves the accuracy of the method of Ref. 1. It is suggested that this correction factor is a universal function of the transonic similarity parameter which, once established, can be used in subsequent calculations. The correction factor is found by using the results of the recent numerical methods[2,3] to locate the shock wave correctly in a number of examples.

Analysis

For a freestream Mach number M_∞ and a transonic parameter k the fundamental integral equation obtained by Spreiter and Alksne[1] for symmetric aerofoils at zero incidence is

$$\bar{u}(x,o) - \frac{\bar{u}^2(x,o)}{2} = \bar{u}_{T_\infty}(x) + g(x,x_s) \tag{1}$$

where $\bar{U}(x,o)$ is related to the surface perturbation velocity in the freestream direction, $U(x,o)$, by

Received July 19, 1973.
Index category: Subsonic and Transonic Flow.
*Senior Research Fellow.

$$\bar{u}(x,o) = \frac{k}{(1-M_\infty^2)}u(x,o) \tag{2}$$

$\bar{U}_{T_\ell}(x)$ is related to the linearised surface perturbation velocity in the freestream direction and is given by

$$\bar{u}_{T_\ell}(x) = \frac{1}{\pi}\int_0^1 \frac{\bar{Z}_T'(\xi)}{(x-\xi)}d\xi \tag{3}$$

where $Z_T(x) = (k/(1 - M_\infty^2)\, Z_T(x)$; $Z = Z_T(x)$ denotes the thickness distribution of the aerofoil. $g(x,x_s)$ is a field integral defined by

$$g(x,x_s) = \lim_{\substack{\epsilon\to 0\\ \delta\to 0}} \left\{ -\frac{1}{4\pi}\left\{ \int_{-\infty}^{x-\epsilon}\left[\int_0^\infty \frac{\partial^2(\ln(r))}{\partial x\partial\xi}\bar{u}^2(\xi,\zeta)d\zeta\right]d\xi \right.\right.$$
$$+ \int_{x+\epsilon}^{x_s-\delta}\left[\int_0^\infty \frac{\partial^2(\ln(r))}{\partial x\partial\xi}\bar{u}^2(\xi,\zeta)d\zeta\right]d\xi +$$
$$\int_{x_s+\delta}^{\infty}\left[\int_0^\infty \frac{\partial^2(\ln(r))}{\partial x\partial\xi}\bar{u}^2(\xi,\zeta)d\zeta\right]d\xi$$
$$+ \int_{-\infty}^{x_s-\delta}\left[\int_{-\infty}^0 \frac{\partial^2(\ln(r))}{\partial x\partial\xi}\bar{u}^2(\xi,\zeta)d\zeta\right]d\xi +$$
$$\left.\left. \int_{x_s+\delta}^{\infty}\left[\int_{-\infty}^0 \frac{\partial^2(\ln(r))}{\partial x\partial\xi}\bar{u}^2(\xi,\zeta)d\zeta\right]d\xi \right\}\right. \tag{4}$$

where $r = [(x - \xi)^2 + \zeta^2]^{1/2}$ and x_s is the shock location. Sonic conditions exist at the surface when $\bar{U}(x,o)$ is unity and the shock location is found by ensuring a finite acceleration at the sonic point; this leads to the following pair of equations for x_s and the sonic point, x_{sonic}.

$$\left.\begin{aligned} \frac{\partial}{\partial x}\{\bar{U}_{T_\ell}(x) + g(x,x_s)\}\Big|_{x=x_{\text{sonic}}} &= 0 \\ \{\bar{U}_{T_\ell}(x) + g(x,x_s)\}_{x=x_{\text{sonic}}} &= 1/2 \end{aligned}\right\} \tag{5}$$

In order to solve Eq. (1) the double integral $g(x,x_s)$ in Eq. (4) needs to be evaluated which requires a knowledge of $\bar{U}(\xi,\zeta)$ over the entire flowfield. Spreiter and Alksne[1] approximated the variation of $\bar{U}(\xi,\zeta)$ with ζ by the following relations.

$$\left.\begin{aligned} \zeta \geq 0,\ \bar{U}(\xi,\zeta) &= \frac{\bar{U}(\xi,0)}{\left[1 - \frac{\bar{Z}_T''(\xi)\zeta}{2\bar{U}(\xi,0)}\right]^2} \\ \zeta \leq 0,\ \bar{U}(\xi,\zeta) &= \frac{\bar{U}(\xi,0)}{\left[1 + \frac{\bar{Z}_T''(\xi)\zeta}{2\bar{U}(\xi,0)}\right]^2} \end{aligned}\right\} \tag{6}$$

Using Eq. (6) in Eq. (4) an approximation to $g(x,x_s)$, denoted by $I[x,x_s, \bar{U}(x,o)]$, can be found where

$$g(x,x_s) \approx I[x,x_s,\bar{u}(x,0)] =$$
$$-\frac{1}{2\pi}\left\{\int_0^{x_s}\bar{U}(\xi,0)\bar{Z}_T''(\xi)E_T\left[\frac{-(x-\xi)\bar{Z}_T''(\xi)}{2\,\bar{U}(\xi,0)}\right]d\xi\right.$$
$$\left. + \int_{x_s}^1 \bar{U}(\xi,0)\bar{Z}_T''(\xi)E_T\left[\frac{-(x-\xi)\bar{Z}_T''(\xi)}{2\bar{U}(\xi,0)}\right]d\xi\right\} \tag{7}$$

and

$$E_T(x) = \frac{1}{(1+x^2)^5}\left\{\frac{(1+x^2)}{6}\times\right.$$
$$\left.(x^6 + x^4 + 71x^2 - 25) - 2(5x^4 - 10x^2 + 1)\ln|x|\right.$$
$$\left. + \pi(5 - 10x^2 + x^4)|x|\right\} \tag{8}$$

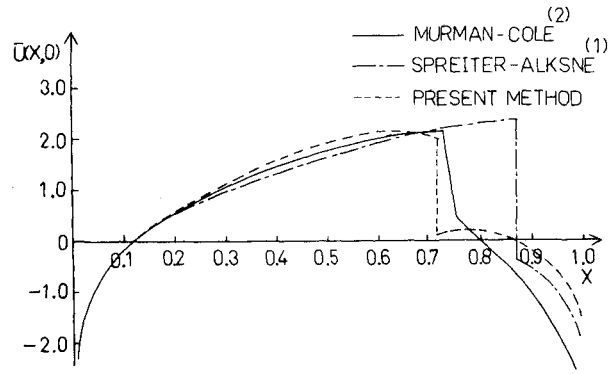

Fig. 1 Surface velocity distribution on a 6% circular-arc aerofoil; $M_\infty = 0.872$.

In Ref. 1 only sharp-nosed aerofoils are considered and the fact that the linear velocity distribution $\bar{U}_{T_\ell}(x)$ is logarithmically singular at the leading edge of sharp-nosed aerofoils does not introduce any difficulties. For round-nosed aerofoils, however, $\bar{U}_T(x)$ has a leading edge singularity of the order of $(x)^{-1/2}$ which when substituted into Eq. (1), leads to an imaginary value of $\bar{U}(x,o)$ near the leading edge: this behavior can be easily eliminated if, for example, $\bar{U}_{T_\ell}(x)$ can be replaced by $\bar{U}_{TL}(x)$[6] where

$$\bar{U}_{T_\ell}(x) = \frac{\bar{U}_{T_\ell}(x)}{\left\{1 + \frac{[Z_T'(x)]^2}{(1-M_\infty^2)}\right\}^{1/2}} +$$
$$\frac{k}{(1-M_\infty^2)}\left[\frac{1}{\left\{1 + \frac{[Z_T'(x)]^2}{(1-M_\infty^2)}\right\}^{1/2}} - 1\right] \tag{9}$$

Substitution of Eqs. (7), (9) into Eq. (1) gives

$$\bar{U}(x,0) - \frac{\bar{U}^2(x,0)}{2} = \bar{U}_{T_\ell}(x) + I[(x,x_s,\bar{U}(x,0))] \tag{10}$$

and the shock location can be found using Eqs. (5), (7), and (9).

The distribution of $\bar{U}(x,o)$ around a 6% circular arc aerofoil at zero incidence when $M_\infty = 0.872$ has been calculated and is shown in Fig. 1 compared to the results of Murman and Cole.[2] In this calculation, as in subsequent calculations, the parameter k is taken to be

$$k = (\gamma + 1)M_\infty^{3/2}$$

where γ is the ratio of specific heats. Although the distributions of $\bar{U}(x,o)$ ahead of the shock agree fairly well, the shock location calculated using the method of Ref. 1 is further aft than the location predicted by Murman and Cole.[2] Both the method of Murman and Cole[2] and the method of Spreiter and Alksne[1] are based on the transonic small disturbance equation and the difference between these two results can be attributed to an inaccurate approximation of $g(x,x_s)$ by $I[x,x_s,\bar{U}(x,o)]$ due to deficiencies in the approximation formulae of Eq. (6). In order to improve the results of the integral method as derived by Spreiter and Alksne[1] some means of improving the accuracy of the approximation to $g(x,x_s)$ must be devised.

It is found that an improved approximation to $g(x,x_s)$ is given by

$$g(x,x_s) = \epsilon I_T(x,x_s,\bar{U}(x,0)) \tag{11}$$

where it is assumed that ϵ is independent of x. Some evidence for the validity of this assumption is given in Fig. 1 where it can be seen that the velocity distribution $\bar{U}(x,o)$

Table 1

Aerofoil	M_∞	χ	x_s	$\epsilon(\chi)$
NACA 0012[a]	0.902	−0.476	0.895	1.56
NACA 0012[b]	0.864	−0.676	0.675	1.50
NACA 0012[c]	0.815	−0.952	0.49	1.45
NACA 0012[c]	0.791	−1.093	0.39	1.43
NACA 0015[a]	0.81	−0.84	0.56	1.48
6% Circular arc[d]	0.909	−0.699	0.84	1.43
6% Circular arc[d]	0.872	−1.01	0.735	1.35

[a]Example quoted in Ref. 3.
[b]Example quoted in Ref. 4.
[c]Examples calculated by the Aircraft Research Association.
[d]Example quoted in Ref. 2.
Values of $\epsilon(\chi)$ for Several Test Cases.

ahead of the shock is given fairly accurately by the method of Ref. 1; this implies that the functional dependence of $g(x,x_s)$ on x is adequately represented by $I[x,x_s,\bar{U}(x,o)]$.

From the similarity laws regarding the transonic flow around affinely related thin aerofoils the velocity distribution $\bar{U}(x,o)$ should remain unchanged provided the transonic similarity parameter, χ, given by

$$\chi = -\frac{(1-M_\infty^2)}{(k\tau)^{2/3}} \tag{12}$$

where τ is the thickness parameter of the aerofoil, remains constant. If χ is unchanged then $\bar{Z}_T''(x)$ is unchanged and hence $I[x,x_s,\bar{U}(x,o)]$, given by Eq. (7), is unchanged. Furthermore to first order in the thickness parameter $\bar{U}_{TL}(x)$ is unchanged and hence it can be implied that ϵ is a function of the similarity parameter χ. The correction factor, ϵ, may also be a function of additional parameters that characterise a particular family of aerofoils but as a first step it is assumed in this analysis that ϵ is a function only of χ. Thus

$$\epsilon = \epsilon(x) \tag{13}$$

Since it has been assumed earlier that $\epsilon(\chi)$ is independent of the chordwise variable it is implied by Eq. (13) that $\epsilon(\chi)$ is the same function of χ whatever the aerofoil under consideration. The main discrepancy in the result of Ref. 1 is in the shock location and it is proposed to find $\epsilon(\chi)$ by reference to the more exact numerical results[2-4] now available to locate the shock wave accurately in a number of examples.

Results

In the results of the numerical methods of Refs. 2-4 the shock wave is represented by a rapid compression and for the present purpose it is assumed that the shock wave lies at the midpoint of this rapid compression.

Seven examples are used and details of the aerofoils and the origin of the data as well as the calculated values of $\epsilon(\chi)$ are given in Table 1.

It is desirable to approximate the correction factor $\epsilon(\chi)$ by some analytic function of χ and this is done by representing $\epsilon(\chi)$ by a second order polynomial in χ and correlating the shock locations to minimise the percentage error; $\epsilon(\chi)$ is found to be given approximately by

$$\epsilon(x) \approx 1.614 + 0.178x + 0.0095x^2 \tag{14}$$

This approximation to $\epsilon(\chi)$ correlates the shock locations in the seven examples to an accuracy of 3%. It is interesting to note that the variation of $\epsilon(\chi)$ with χ is relatively small.

Having located the shock wave fairly accurately the corresponding pressure (or velocity) distributions can be determined.

The pressure distribution (p/p_o), where p_o is the stagnation pressure, for the flow around a NACA 0012 aerofoil at $M_\infty = 0.864$ (one of the seven examples) is shown in Fig. 2 and is compared to the pressure distribution found by Steger and Lomax.[4] The present results compare favourably with those of Steger and Lomax except in the immediate vicinity of the shock where the pre-shock compression and the post-shock expansion predicted by Oswatitsch and Zierup[5] is evident.

In addition the velocity distribution $\bar{U}(x,o)$ over the 6% circular arc aerofoil at $M_\infty = 0.872$ has been calculated and is shown in Fig. 1 for comparison with the results of Ref. 1 and Ref. 2. The present results compare well with those found by Murman and Cole[2] ahead of the shock wave but behind the shock there is substantial disagreement. The reason for this disagreement is not clear but at least the present results give the correct shock jump relations.

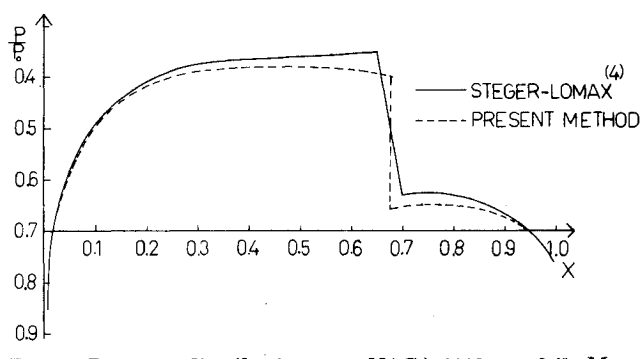

Fig. 2 Pressure distribution on a NACA 0012 aerofoil; M_∞ = 0.864

References

[1]Spreiter, J. R. and Alksne, A., "Theoretical Prediction of Pressure Distributions on Non-Lifting Airfoils at High Subsonic Speeds," TN 3096, 1954, NACA.

[2]Murman, E. and Cole, J. D., "Calculation of Plane Steady Transonic Flows," *AIAA Journal*, Vol. 9, No. 1, Jan. 1971. pp. 114-121.

[3]Murman, E., "Computational Methods for Inviscid Transonic Flows with Imbedded Shock Waves," *Numerical Methods in Fluid Dynamics*—AGARD LS-48 1972, Chap. 13.

[4]Steger, J. L. and Lomax, H., "Numerical Calculation of Transonic Flows about Two-Dimensional Airfoils by Relaxation Procedures," AIAA Paper 71-569 June 1971,

[5]Oswatitsch, K. and Zierup, J., "Das Problem des senkrechten stosses an einer gekrummten Wand," Zeitschrift fur Angewandt Mathematik und Mechanik, Vol. 40 1960, pp. 143-144.

[6]Nixon, D. and Hancock, G. J., "High Subsonic Flow Past a Two-Dimensional Aerofoil," Rept. QMC-EP 1000 1972, Queen Mary College, London, England.

An Optimized Video Output from a Wide Angle Optical Probe

J. A. Mays* and R. E. Holmes†
Systems Research Laboratories, Inc., Dayton, Ohio

THE current and future requirements for Aircraft/Aerospace Visual Simulators demands ever increasing resolution. This is necessary in order that existing simulation

Submitted as Paper 73-918 at the AIAA Visual and Motion Simulation Conference, Palo Alto, Calif., September 10-12, 1973; received September 26, 1973; revision received November 26, 1973. Acknowledgement is made to Mr. C. F. McNulty, Chief of the Simuationa Techniques Branch, Air Force Human Resources Laboratory, WPAFB, Dayton, Ohio, and to Mr. A. T. Gill, Contract Monitor, for their assistance, cooperation, and consultation throughout the program.

Index categories: Aircraft Crew Training; Spacecraft Ground Testing and Simulation (Including Components).

*Staff Video Engineer, Electronic Image Systems Group.
†Manager Electronic Image Systems Group.